ELEVENTH INTERNATIONAL CONFERENCE ON INTERGRANULAR AND INTERPHASE BOUNDARIES 2004

JOURNAL OF MATERIALS SCIENCE **40** (2005) 3219–3223

Energies of [001] small angle grain boundaries in aluminum

A. OTSUKI
Institute of Advanced Energy, Kyoto University, Uji, Kyoto, 611-0011, Japan

Energies of symmetric [001] tilt and twist small angle grain boundaries in aluminum have been examined as a function of misorientations. Boundary energies were evaluated relative to solid/liquid interfacial energies by a dihedral angle method on surface grooves. Energies of $(100)_s$ tilt boundaries with the Burgers vector of a[100] were rather smaller than those of $(110)_s$ tilt boundaries with $a/2$[110]. Energies of twist boundaries at $\theta < 4^\circ$ were slightly larger than those of $(110)_s$ tilt boundaries. The energies were well explained as a function of misorientations by the Read-Shockley type equation. The equation also correctly described the difference in elastic energy factors between the $(110)_s$ tilt and twist boundaries. However, the term b in the equation may take a constant value independent of the Burgers vectors.

1. Introduction

The most acceptable structure model of small angle grain boundaries is the dislocation model. Read and Shockley [1] introduced the dislocation model for energies using the elastic theory. Boundary energies, γ_{gb}, are described as a function of the misorientation, θ as,

$$\gamma_{gb} = E_0\theta(A_0 - \ln\theta), \tag{1}$$

$$E_0 = \frac{\mu b}{4\pi(1-\nu)}, \quad \text{for tilt}, \quad E_0 = \frac{\mu b}{2\pi}, \quad \text{for twist}.$$

E_0 is the constant as the function of the elastic modulus, μ, the magnitude, b, of the Burgers vector, **b**, and Poisson ratio, ν. A_0 is the constant as a function of the core radius of boundary dislocations. Although the Read-Shockley Equation 1 was originally introduced for the elastic energies, boundary energies including core energies may be described by the Read-Shockley equation [2].

To examine the Read-Shockley model experimentally, many examinations have been performed [3–5]. Energies of Al small angle boundaries were also well expressed by the equation [6]. The equation means that energies depend on the magnitude of the Burgers vector of boundary dislocations. However, energies of Al [001]$(100)_s$ tilt small angle boundaries with the Burgers vector of a[100] were found to be smaller than those of $(110)_s$ boundaries with the Burgers vector of $a/2$[110] [6–8]. (The expression (100)s or (110)s boundaries mean that the boundaries are in a symmetrical position between the (100) or (110) planes of crystal 1 and crystal 2.) These studies required further examinations of small angle boundaries to check with the Read-Shockley model.

In the present study, experimental results for energies of [001] tilt and twist small angle boundaries in aluminum are reported. These boundaries allow us to compare among energies with respect to elastic moduli and the Burgers vector.

2. Experimental procedures

To examine boundaries with the desired misorientations, bicrystals of 99.999% pure aluminum were grown from the melt, using seed crystals. Bicrystals were used in the deviation within 2° from the [001] orientation. The misorientation angle is denoted by the angle, θ, made by each [010] orientation. Thus, small angle boundaries near $\theta = 0^\circ$ indicate $(100)_s$ tilt small angle boundaries, while boundaries near $\theta = 90^\circ$ indicate $(110)_s$ tilt small angle boundaries. Grain boundary energies were obtained by measuring dihedral angles of surface grooves at boundaries; the ratio of the grain boundary energy, γ_{gb}, to the solid/liquid interfacial energy, $2\gamma_{sl}$, is correlated with the dihedral angle, α, as follows (Fig. 1),

$$\gamma_{gb}/2\gamma_{sl} = \cos(\alpha/2). \tag{2}$$

This equation assumes that crystallographic anisotropy in the γ_{sl} is negligible [9], since the anisotropy in surface energy of aluminum was found to be less than 5% [10]. Also the grain boundary torque term is neglected, because the boundaries did not migrate from a position normal to solid/liquid interfaces. To form surface grooves, aluminum specimens were wetted with Sn-20 mass%Zn alloy, pre-heattreated at 673 K for 1 h, and then treated at 513 K for 2 days in a vacuum capsule. This two step heat treatment was done to protect as much as possible the occurrence of the grain boundary migration induced with the diffusion of Zn atoms into aluminum boundaries from the melt [11]. The equilibrium concentration of Zn in the Sn-Zn liquid phase is 12.5%Zn at 513 K [12]. Indeed, the Al(solid)/SnZn(liquid) interfacial energy depended on

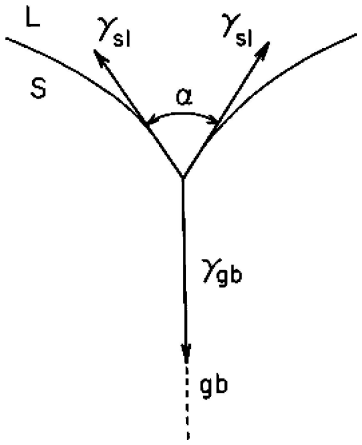

Figure 1 Interfacial energy balance at an intersection of solid/liquid interfaces and a grain boundary.

the Zn concentration in the liquid metal [13]. The Zn equilibrium concentration in the liquid phase was maintained using a high Zn concentration of the Sn20%Zn alloy during the heat treatment. Consumed Zn in the liquid phase diffusing into aluminum was supplied from solid phase Zn in the Sn20Zn alloy. Aluminum has solid solubility of about 10 mass.%Zn at 513 K [12]. Thus, the boundary energy measured in this experiment referred to that of the Al-Zn alloy instead of pure Al. A typical shape of a boundary groove profile formed at an aluminum(solid)/Sn20Zn(liquid) interface after the heat treatment is shown in Fig. 2. The grain boundary is traced by a broken line. The profile of the solid(s)/liquid(l) interface was smooth and did not show facetting. The obtained mean values of α are shown together with 90% confidence limits using the t-distribution in the statistics.

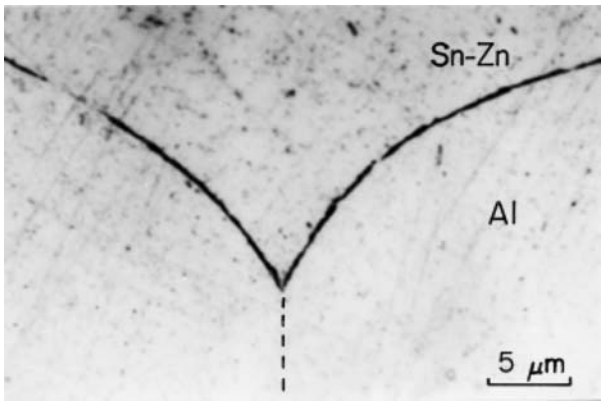

Figure 2 A boundary groove formed at an Al/Sn20%Zn interface.

3. Results and discussion

Figs. 3a and b show the dependence of the experimentally obtained dihedral angle α for the $(100)_s$ and $(110)_s$ tilt boundaries on misorientation angles, respectively. (Note that θ for $(110)_s$ tilt boundaries was marked from 90° to 70° indicating misorientations of their small angle boundaries.) The scale on the right hand is marked in the relative boundary energies $\gamma_{gb}/2\gamma_{sl} = \cos(\alpha/2)$. Boundary energies increased with increasing misorientation. The energies of twist boundaries (Fig. 3c) were slightly larger than those of $(110)_s$ tilt boundaries in the range of $\theta < 4°$ and smaller than those of tilt boundaries in the range of $\theta > 4°$. A similar experimental result has also been reported in examinations using triple junction geometry in aluminum by Yang *et al.* [5]. Scattered data observed at coincidence boundaries in larger θ, corresponding to energy cusps.

Since the Read-Shockley equation is described by two factors of E_0 and A_0, the difference between the energies of $(100)_s$ and $(110)_s$ tilt boundaries could not be explained simply. To examine the effect of the E_0 and A_0 terms separately, Equation 1 is combined with Equation 2 to use the dihedral angle measurements, as

$$\frac{\gamma_{gb}}{2\gamma_{sl}\theta} = \frac{\cos(\alpha/2)}{\theta} = \frac{E_0}{2\gamma_{sl}}(A_0 - \ln\theta) = S_0(A_0 - \ln\theta). \quad (3)$$

Fig. 4 shows the relationship of the $\cos(\alpha/2)/\theta$ vs. $\ln\theta$ for the $(110)_s$ boundaries. (For these boundaries, note that θs in both the terms of $\cos(\alpha/2)/\theta$ and $\ln\theta$ are substituted by $\theta' = 90°–\theta$, because $\theta = 90°$ to 70° corresponds to misorientations of the small angle

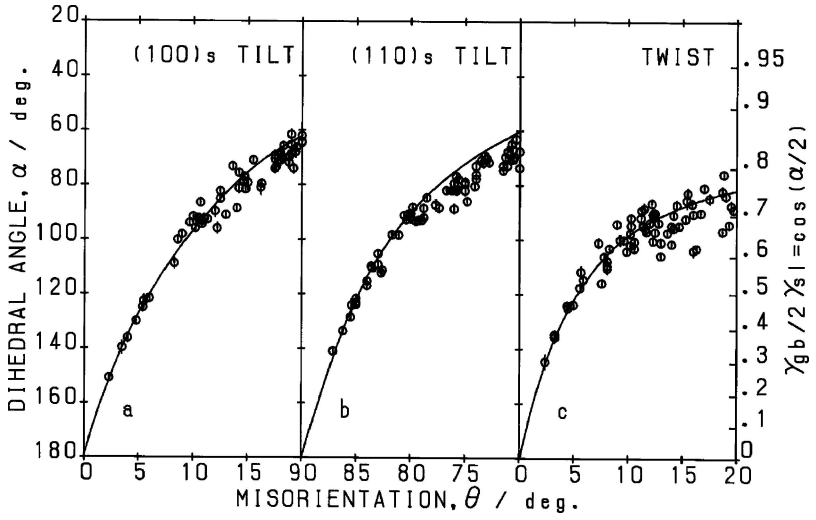

Figure 3 Dihedral angle variation with θ, (a) 0–20°$(100)_s$ tilt, (b) 70–90°$(110)_s$ tilt and (c) twist boundaries.

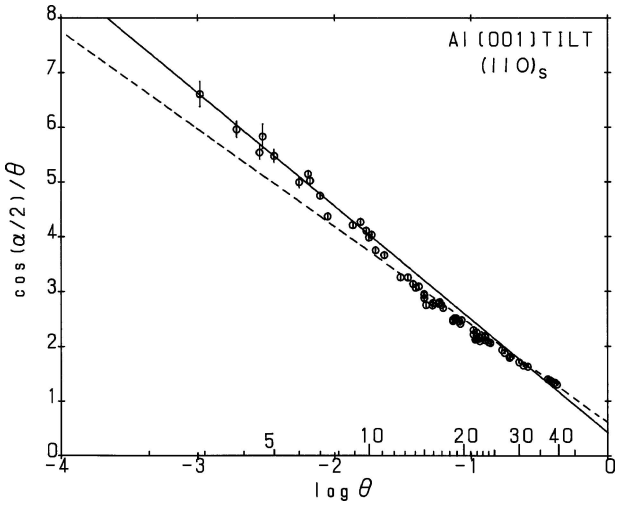

Figure 4 Read-Shockley analyses on energies of small angle boundaries, the solid line for $(110)_s$ and dotted line for $(100)_s$ tilt boundaries.

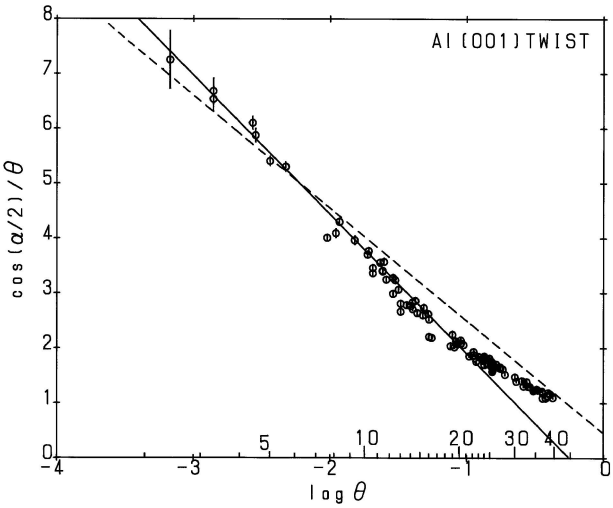

Figure 5 Read-Shockley analyses on energies of small angle twist boundaries, the solid line for twist and dotted line for $(110)_s$ tilt boundaries.

boundaries as seen in Fig. 3b.) The measurements of the region of $\theta' = 3^\circ$ to 10° are represented by a linear relation following Equation 3. This suggests that the energies of small angle boundaries are described by the Read-Shockley equation [1]. The dotted line in Fig. 4 shows the $(100)_s$ boundaries. The slope of the dotted line is smaller than that for $(110)_s$ tilt boundaries. Slopes and intersections on the $\ln\theta$ axis in the linear lines indicate the $S_0 = E_0/2\gamma_{sl}$ and A_0 values, respectively. S_0 and A_0 values obtained using the least squares estimation are summarized in Table I. Here, data points regarded as energy cusps were eliminated in the least squares estimation. S_0 values of $(100)_s$ and $(110)_s$ boundaries were 1.78 ± 0.09 and 2.07 ± 0.16, respectively. In contrast, the A_0 value for the $(100)_s$ boundaries was rather larger than that for the $(110)_s$ boundaries. Therefore, the lower boundary energies of $(100)_s$ boundaries were due to the small E_0 value, because the γ_{sl} may take a constant value independent of surface orientation [10].

Fig. 5 shows the relationship of the $\cos(\alpha/2)/\theta$ vs. $\ln\theta$ for the twist boundaries. The measurements of the region of $\theta = 2^\circ$ to 10° were also represented by a linear relationship following equation 3. The slope of the solid line was larger than that of the dotted line for the $(110)_s$ tilt boundaries. The measured S_0 and A_0 values were 2.53 ± 0.05 and -0.25 ± 0.03, respectively, as shown in Table I.

TABLE I Read-Shockley analyses

g.b.	$S_0 = E_0/2\ \gamma_{sl}$	S_{0t}/S_{0w}	$A_\circ$
Tilt $(100)_s$	1.78 ± 0.09	0.70	0.36 ± 0.10
Tilt $(110)_s$	2.07 ± 0.16	0.82	0.20 ± 0.17
Twist	2.53 ± 0.05		-0.25 ± 0.03

g.b.	**b**	$K \times 10^{11}$ Nm^{-2}	$H \times 10^{10}$ Nm^{-2}	H_t/H_w	E_0 (Jm^{-2})	γ_{sl} (mJm^{-2})
Tilt $_s$	$a\langle 100\rangle$	0.3473	0.2764	0.777	1.125	316
$(100)_s$		$(\sim \mu/(1\text{-}\nu))$	$(K/4\pi)$			± 10
Tilt$_s$	$a/2\langle 110\rangle$	0.3621	0.2882	0.810	0.8296	200
$(110)_s$		$(\sim \mu/(1\text{-}\nu))$	$(K/4\pi)$			± 17
Twist	$a/2\langle 110\rangle$	0.2235	0.3556		1.024	202
(001)		$(\sim \mu)$	$(K/2\pi)$			± 6

3.1. Comparison between the energies of $(110)_s$ tilt and twist boundaries

E_0 is the energy factor dependent on the dislocation structure according to the Read-Shockley equation. The Burgers vector **b** for the $(110)_s$ boundaries in aluminum was found to be $a/2[110]$ from the dislocation spacing in the direct observation by Shamsuzzoha *et al.* [14]. (The quantity of "a" is the lattice constant.) They also concluded that dislocations were 90° pure edge dislocations. The Burgers vector of (001) twist boundaries of aluminum was also observed to be $a/2\langle 110\rangle$ by Wagner and Balluffi [15]. Because both the Burgers vectors of $(110)_s$ tilt and (001) twist boundaries were equal, the obtained ratio S_{0t}/S_{0w} should represent the ratio of $H_t/H_w = K_t/2K_w$. K is the energy factor for dislocations: $K_t \cong \mu/(1\text{-}\nu)$ for tilt boundaries and $K_w \cong \mu$ for twist boundaries. K was calculated by Steed's equation [16] using the elastic constants of $C_{11} = 0.9820$, $C_{12} = 0.5844$ and $C_{44} = 0.2512 \times 11^9\ \mathrm{Nm}^{-2}$ measured by Gerlich and Fisher [17]. The effect of the elastic anisotropy on the energy factor K was considered. S_{0t}/S_{0w} of 0.82 shown in Table I was in good agreement with $H_t(110)_s/H_w = 0.81$. This suggests that energies of Al $(110)_s$ tilt and (001) twist small angle boundaries were well explained by the Read-Shockley equation [1].

3.2. Comparison between the energies of $(100)_s$ and $(110)_s$ tilt boundaries

On the $(100)_s$ boundaries, we obtained the value of $S_0 = E_0/2\gamma_{sl}$ of 1.78 ± 0.09 smaller than 2.07 ± 0.16 for $(110)_s$ boundaries as shown in Table I. Dislocations in the $(100)_s$ boundaries were found to possess $\mathbf{b} = a[100]$ from dislocation spacing by Liu and Balluffi [18]. If the dislocations are pure 90° edge dislocations, the energy factor $K_t(100)_s$ value is not so different from K_t $(110)_s$ as shown in Table I. Thus, the E_0 value of the $(100)_s$ boundaries is expected to be $\sqrt{2}$ times larger than

TABLE II Core models for a[100] dislocations

Model	decomposition or dissociation	K_d(eq.)	K(value) $\times 10^{11}$ Nm^{-2}
(a)	no decomposition a[100] on (010)	K_{e1}	0.3473
(b)	two edge dislocations $a/2[110] + a/2[1\bar{1}0]$ on {110}	$2\frac{1}{2}K_{e2}$	0.3473
(c)	partial dislocations $a/2[100] + a/2[100]$ on (010)	$2\frac{1}{4}K_{e1}$	0.1736
(d)	45° mixed dislocations $a/2[101] + a/2[10\bar{1}]$ on (010)	$2\frac{1}{4}(K_{e1} + K_s)$	0.2992

Model	b_d	b_d^2 ($b = a$)	$E_0(b' = a/\sqrt{2})$ (Jm^{-2})	E_0/E_0 (110)	γ_{sl} (mJm^{-2})
(a)	a	a	0.7956	0.959	223
(b)	a/$\sqrt{2}$	a/2	0.7956	0.959	223
(c)	a/2	a/4	0.3978	0.480	112
(d)	a/$\sqrt{2}$	a/2	0.7404	0.892	208

that of $(110)_s$ boundaries following the magnitudes of the Burgers vectors of a[100] for $(100)_s$ and $a/2$[110] for $(110)_s$ boundaries as shown in Table I. However, the obtained $E_{0t}(100)_s/E_{0w} = 1.099$ was much larger than $S_{0t}(100)_s/S_{0w} = 0.70$. For this reason, it seems that the $(100)_s$ boundaries do not consist of 90° pure edge dislocations.

The observation of dislocation cores of the $(100)_s$ tilt boundaries has shown that the dislocations had an elongated form with two separate cores [19, 20]. To explain the elongated cores, the models proposed for [001]$(100)_s$ tilt boundaries are as follows;

(a) no decomposition, 90° pure edge dislocations [21],
(b) decomposition into two $a/2\langle 110\rangle$ edge dislocations [19, 21],
(c) dissociation into two $a/2$[100] pure edge dislocations [22],
(d) decomposition into two $a/2\langle 110\rangle$ 45° mixed dislocations [20],
(e) serration and dissociation [23].

Darby and Balluffi [23] observed a serrated dislocation structure in Au [001]$(100)_s$ tilt boundaries and proposed model (e). However, the dislocations in Al [001]$(100)_s$ tilt boundaries were observed to be straight by Liu and Balluffi [18]. For models from (a) to (d), calculated K values are shown in Table II.

Here, K_e and K_s are the energy factors for edge and screw dislocations, respectively and were calculated for dislocations on each plane as shown in Table II [16] : $K_{e1} = K_{e2} = 0.3473$ and $K_s = 0.2512$. The energy γ_{gb} of boundaries consisting of decomposed dislocations in aluminum may be described as similar to the Read-Shockley equation (see Appendix I), as

$$\gamma_{gb} = (K_d/4\pi)\left(b_d^2/b\right)\theta(A_0 - \ln\theta) = (K_d/4\pi)b'\theta(A_0 - \ln\theta), \quad (4)$$

where K_d is the energy factor for decomposed dislocations, and b and b_d are the magnitudes of the Burgers vector of non-decomposed and decomposed dislocations, respectively. In the case of $b = a$ for $\mathbf{b} = a$[100], calculated b_d^2/b were too small to explain the experimental results except model (a), while E_0 obtained from model (a) was too large as mentioned above as shown in Table II. Therefore, it is assumed that the term b in equation 1 for $(100)_s$ may take $a/\sqrt{2}$ as same as that of $(110)_s$, because it seems that both S_0 values were rather similar. The term b in Equation 1 corresponds to the term $b' = b_d^2/b$ in Equation 4. Using $b' = a/\sqrt{2}$, calculated K, E_0 and γ_{sl} values were shown in Table II. The ratio of $E_0/E_0(110)_s = 0.959$ for models (a) and (b) was larger than the ratio of $S_0(100)_s/S_0(110)_s = 1.78/2.07 = 0.869$. On the other hand, $E_0/E_0(110)_s = 0.892$ value for model (d) showed an approximately equal value of $S_0(100)_s/S_0(100)_s = 1.787/2.07 = 0.869$. This suggests that the boundary structure of $(100)_s$ tilt boundaries may consist of 45° mixed dislocations shown by model (d). To confirm this result, further examinations on the dislocation core structure are desirable in future.

This conclusion was due to the assumption that the term b in E_0 took the same value as that of $(110)_s$, corresponding to the nearest interatomic distance of fcc crystals. Similar results were already found, in that the misorientation dependence of $\Sigma = 3$ boundary energies was explained by the term b corresponding to the magnitude of $a/2\langle 110\rangle$ independent of the Burgers vector of secondary dislocations of $b = 1/3\langle 111\rangle$ for these boundaries [13]. In addition, Tsurekawa *et al.* [24] pointed out that energies of small to large angle boundaries may be described by the Read-Shockley type equation as a function of the boundary dislocation density, b/D, instead of θ, where D is the dislocation spacing. They also found that the factor E_0 may be constant independent of the Burgers vectors. This suggests that small angle boundaries consisting of dislocations with any given Burgers vector show macroscopically equal elastic strain fields independent of the Burgers vector. The net Burgers vector, **B**, of boundary dislocations is given by Frank's formula for small angle boundaries [2]. If boundaries consist of dislocations with Burgers vector $\mathbf{b_i}$, $\mathbf{B} = \Sigma n_i \cdot \mathbf{b_i}$, where n_i is the number of dislocations with Burgers vector $\mathbf{b_i}$. In the case of boundaries consisting of one kind of dislocations, the net Burgers vector **B** is only given by θ, $\mathbf{B} = 2\sin(\theta/2) \sim \theta$. Therefore, in other words, small angle boundaries at any misorientation θ show macroscopically equal elastic strain fields independent of the Burgers vectors. In future, it will be desirable to introduce a new model to describe small angle boundary energies.

3.3. Evaluation of Al (solid)/Sn-Zn (liquid) interfacial energies

To obtain absolute boundary energies of aluminum, the γ_{sl} values are calculated by substituting E_0 values into the $S_\circ$ values. For this purpose, the value of the term b in E_0 must be determined appropriately. For $(110)_s$ tilt and twist boundaries, assuming $b = a/\sqrt{2}$ (a = 0.4071 nm) at 513 K, γ_{sl} values were estimated to be 200–202 m^{-2} as shown in Table I. Using the γ_{sl} value, absolute energies of Al [001] boundaries were given by substituting this value in the right hand vertical axis

in Fig. 3. This figure shows that the energies of high angle tilt boundaries are roughly 360–370 mJ·m^{-2} at 513 K. Empirically, boundary energies are well known to be roughly equal to one third of the surface energy of a solid phase itself. The surface energy of Al has been measured to be 1100 mJ·m^{-2} [25] at 513 K, and the γ_{gb} was estimated to be 370 mJ·m^{-2}, agreeing well with this observation. On the other hand, energies of twist boundaries are about 310 m^{-2} and smaller than those of tilt boundaries. In addition, in experiments for the temperature dependence of boundary energies in aluminum, the γ_{sl} value estimated using $b = a/\sqrt{2}$ was extrapolated at the melting point of Al and showed good agreement with pure aluminum solid/liquid interfacial energies [26]. Therefore, it seems to be reasonable that the term b takes the value of the nearest interatomic distance.

4. Summary

The boundary energies of symmetric [001] tilt and twist small angle boundaries in aluminum were measured at 513 K. The results are summarized as follows :

1. The small angle boundary energies were well explained by the Read-Shockley type equation.
2. The slope S_0 for (001) twist boundaries was larger than that for $(110)_s$ tilt boundaries. This result was consistently explained by the difference of the elastic constants.
3. The slope S_0 of $(100)_s$ tilt boundaries with the Burgers vector of $a\langle 100\rangle$ was slightly smaller than that of $(110)_s$ tilt boundaries with Burgers vector of $a/2\langle 110\rangle$.
4. From result 3, it was concluded that the term b in E_0 may take a constant value independent of the Burgers vector. The small S_0 value for $(100)_s$ tilt boundaries may be explained by the decomposed 45° $a/2\langle 110\rangle$ dislocations.

Appendix I [16]

The total energies of decomposed dislocations with width d_s is given as

$$E = 2E_d + E_{12} + \gamma_s d_s,$$
$$E_d = \frac{K_d b_d^2}{4\pi} \ln \frac{R}{r_\circ},$$

where E_d is the energy of a decomposed dislocation, E_{12} the interaction energy between the two decomposed dislocations and γ_s the stacking fault energy [18]. The subscript d indicates decomposed dislocations. $r_\circ$ is the core radius of dislocations. The third term, $\gamma_s d_s$, is the the energy increase resuting from the stacking fault energy, γ_s, added where decomposed dislocations are partial dislocations.

Because the stacking fault energy in aluminum is large, $\gamma_s \sim 200$ mJm^{-2} [27] and d_s is smaller than the dislocation spacing, E_{12} may be independent of θ. Thus, the terms E_{12} and $\gamma_s d_s$ are included into the A_0 term in equations 1 or 3. According to the model introducing the Read-Shockley equation [1], the boundary energies may be described as,

$$\gamma_{gb} = \frac{K_d}{4\pi} \frac{b_d^2}{b} \theta(A_0' - \ln\theta) = \frac{K_d}{4\pi} b'\theta(A_0' - \ln\theta),$$

where b is the magnitude of the Burgers vector of non-decomposed dislocations.

References

1. W. T. READ and W. SHOCKLEY, *Phys. Rev.* **78** (1950) 275.
2. J. P. HIRTH and J. LOTHE, in "Theory of Dislocations" (John-Wiley, 1982).
3. K. T. AUST and B. CHALMERS, *Proc. R. Soc. Lond.* **A204** (1950) 359.
4. N. A. GJOSTEIN and F. N. RHINES, *Acta Metall* **7** (1959) 319.
5. C.-C.YANG, A. D. ROLLETT and W. W. MULLINE, *Scr. Mater.* **44** (2001) 2735.
6. A. OTSUKI and M. MIZUNO, in Proc. 4th. JIM Int. Symp. on Grain Boundary Structure and Related Phenomena, Trans. JIM. Supp., (1986) Vol. 27, p. 789.
7. A. OTSUKI, H. YATO and I. KINJYO, *Material Sci. Forum* **126–128** (1993) 285.
8. A. OTSUKI, *Material Sci. Forum* **207–209** (1996) 413.
9. C. HERRING, "Physics of Powder Metallurgy", (McGraw-Hill N.Y., 1951) p. 143.
10. R. S. NELSON, D. J. MAZEY and R. S. BARNES, *Phil. Mag.* **11** (1965) 91.
11. A. OTSUKI, *Diff. Defect Forum* **126–217** (2003) 149.
12. H. HANSEN, 1958, in "Constitution of Binary Alloys", (McGraw-Hill, N.Y., 1958).
13. A. OTSUKI, Thesis, Kyoto University, 1990.
14. M. SHAMSUZZOHA, M. SMITH and M. DEYMIER, *Script Metall.* **24** (1990) 1611.
15. W. R. WAGNER and R. W. BALLUFFI, *Phil. Mag.* **30** (1974) 679.
16. J. W. STEEDS, in "Introduction to Anisotropic Elasticity Theory of Dislocations", (Clarendon Press, Oxford, 1973).
17. D. GERLICH and E. S. FISHER, *J. Phys. Chem. Solids.* **30** (1969) 1197.
18. L. S. LIU and R. W. BALLUFFI, *Phil. Mag.* **52A** (1985) 713.
19. M. D. VAUDIN, M. RÜHLE and S. L. SASS, *Acta metall* **31** (1983) 1109.
20. S. D' ANTERROCHERS and A. BOURRET, *Phil. Mag.* **49** (1984) 53.
21. T. SCHOBER and R. W. BALLUFFI, *Phys. Stat. Sol.* **(b)44** (1971) 103.
22. D. A. SMITH, V. VITEK and R. C. POND, *Acta Metall* **25** (1977) 475.
23. T. P. DARBY and R. W. BALLUFFI, *Phil. Mag.* **36** (1977) 53.
24. S. TSUREKAWA, K. MORITA, H. NAKASHIMA and H. YOSHINAGA, *Mater. Trans. JIM.* **38** (1997) 393.
25. K. H. WESTMACOTT, R. E. SMALLMAN and P. S. DOBSON, *Metal Sci. J.* **2** (1968) 177.
26. A. OTSUKI, in Int. Conf. on Interface Science and Materials Interconnection, Proceedings of JIMIS-8, Japan Institute of Metals, (1996) p. 323.
27. R. L. FULLMAN, *J. Appl. Phys.* **22** (1951) 448.

Received 9 November 2004
and accepted 31 January 2005